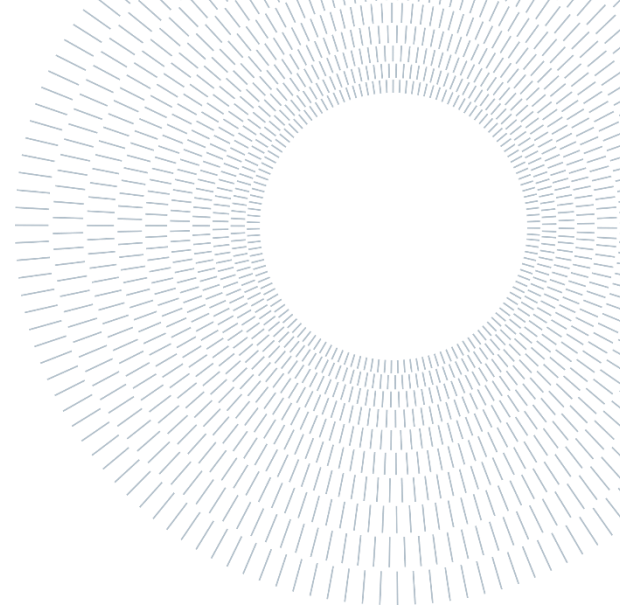




POLITECNICO
MILANO 1863

SCUOLA DI INGEGNERIA INDUSTRIALE
E DELL'INFORMAZIONE



EXECUTIVE SUMMARY OF THE THESIS

Statistical Shape Modelling of the human nasal cavity and CFD simulations

DOUBLE MASTER'S DEGREE IN MECHANICAL AND BIOMEDICAL ENGINEERING
– INGEGNERIA MECCANICA E BIOMEDICA

AUTHOR: Silvia Tonghini

ADVISOR: Prof. Giorgio Colombo

CO-ADVISOR: Prof. Andrea Aliverti, Prof. Michele Bertolini, Prof. Marco Rossoni

ACADEMIC YEAR: 2023-2024

1. Introduction

The nasal cavity plays a crucial role in olfaction. At the top of the nasal cavity lies a specific region called the olfactory epithelium. This area contains millions of olfactory receptor neurons. Malfunctioning of the olfactory system can lead to malnutrition due to the distorted sense of smell and taste, which may reduce pleasure from eating. Moreover, olfaction plays a crucial role in human safety, alerting to dangers like gas leaks, rotten food, or fire. After the global epidemic of SARS-CoV-2, research in this field has gained considerable importance. Several conditions, such as hyposmia and anosmia, remain a significant problem in otolaryngology and neurology in terms of treatment.

This work is part of the ROSE European project, whose goal is to develop a proof of concept that combines miniaturized odour sensors and stimulation arrays, to be evaluated in patients with olfactory disorders.

An innovative tool to investigate deeply anatomical or physiological factors and to develop advanced treatments is the study of computational fluid dynamics (CFD). Through CFD simulations it is possible to investigate nasal cavity dynamics without invasive procedures. Since it is not possible to perform simulations on each patient's anatomy, the development of a statistical shape model (SSM) becomes a real need in medical research. A SSM represents a wide range of variability within a population that can be studied instead of analysing every single patient. Furthermore, starting from a SSM is possible to generate new models, that represent the population, and perform various analyses on them.

The primary aim of this thesis is the development of a SSM of the nasal cavity, including the paranasal sinuses.

The second part of this thesis presents a study of airflow dynamics inside the nose. CFD simulations have been computed to validate the model comparing the results with the literature and introduce a preliminary study of airflow through the nose when introducing a small sensor inside the nostrils.

2. State of art

2.1. Nasal cavity modelling

Several studies in literature have developed virtual models of the nasal cavity but just a few included the paranasal sinuses. An example is the complete model made by Dmitry Tretiakow et al. [1] which has been obtained by manual segmentation of the nasal cavity.

Another similar example is the study of Jan Brüning et al. [2], who also developed a SSM based on 25-symptom-free subjects excluding all the sinuses.

There are many tools for CT scan segmentation. An example of an interesting research about those is the one of Zhang C. et al. [3], who investigated the precision of three different tools to reproduce the nasal model. They replicated the same model with different software, and they concluded that Airway Segmentor (AS) and MIMICS 19.0 (Materialise, Leuven, Belgium) show almost identical and clinically excellent accuracy, while INVIVO 5 (Anatomage, San Jose, CA, USA) reaches a substantially lower precision, with greatly overestimated volumes.

2.2. Statistical shape models (SSM)

Statistical shape models (SSMs) are geometric models that describe a collection of similar objects in a very compact manner. They represent the average shape of many three-dimensional objects as well as their shape variation. Establishing a standard of normality for an anatomical structure requires a comprehensive examination of its range of morphological variations to enhance diagnostic and therapeutic effectiveness. These models represent the probability of specific shapes to occur by the definition of a mean shape and a hierarchy

of primary modes that describe the major trends in shape variation. Moreover, since the obtained shapes are strongly correlated to their geometric representation, they exhibit a generative power.

In the article written by William Keustermans et al. [4], a high-quality statistical shape model of the nasal cavity was built based on a population of nasal shapes. It was shown that such a high-quality model can be used to examine the morphological variations exhibited by the underlying population and relate nasal shape with other metadata such as age and gender. The limit of this study was the exclusion of the paranasal sinuses. The model focuses only on the nasal cavity, and the authors did not apply the model for further study, such as airflow dynamics. Moreover, it's also important to point up that, when considering a SSM, a relevant parameter for understanding the accuracy of the model, is the number of single cavities used to generate it. There is not a threshold number of samples to generate it, but by increasing the cavities, the model becomes much more general and representative of a wider range of human anatomy. In their study, William Keustermans et al. [5], studied a high-quality statistical shape model of the human nose based on CT data of 46 patients. The method presented in their work is based on cylindrical parametrization, which shows great ability to capture and report the natural anatomical variations present in the nasal cavity.

2.3. Computational fluid dynamics (CFD)

In the literature, there are some studies on CFD simulations of the nasal cavity. For example, Guanxia Xiong et al. [6] investigated airflow velocity, trace, distribution, and air pressure, as well as the airflow exchange, between the nasal cavity and paranasal sinus. The velocity field reaches much higher values through the cavity, while is nearly negligible in the other regions. The same can be concluded for the pressure drop. Moreover, the major airflow forms in the nasal cavity are straight in the lower common and inferior meatus, while are parabolic in the middle and upper common meatus. The same considerations have been achieved by Jie Tan et al. [7], who performed turbulent simulation (using the $k-\epsilon$ model) on Chinese adults' noses with normal nasal structure and function.

Most articles exclude the paranasal sinuses from simulations due to their little influence, obtaining a lower computation cost and an easier model to generate, as in the work of Wang Xiao et al. [8]. The choice of the boundary conditions has a high influence on the outputs. To reproduce a realistic situation, a variable pressure drop between the inlet and the outlet is often applied. Moreover, a velocity field and/or a mass flow rate can be introduced. All the reviewed articles include no-slip and rigid walls as boundary conditions applied on the surface of the cavity.

3. Materials and method

3.1. Segmentation

This work started with the CT scan manual segmentation of 40 patients, selected from a pool of 58. This process has been computed on the software MIMICS 24.0 (Materialise, Leuven, Belgium), applying several tools, such as “Threshold”, “Region Growth”, “Split Mask”, “Edit Mask”, etc. The cavity has been separated from each type of sinuses.

This passage has been iteratively done for 40 patients and, for each one, a check of the borders has been made to be sure that the parts were correctly separated and did not overestimate the real dimension of the cavities. Then, a post-process on 3-Matic (Materialise, Leuven, Belgium) has been necessary to generate a unique model through “Boolean Operation”, to fill holes, and to smooth the surface.

3.2. Statistical shape modelling

After meshing all the models with an “Adaptive Surface Mesh”, the fine registration has been performed through the Iterative Closest Point (ICP) algorithm, exposed by 3-Matic through the “Global Registration” function. The procedure has been applied systematically between the reference mesh and all the other 39 cavities. A uniform re-mesh was then applied to the chosen reference, setting a 2mm maximum edge length. This re-meshed cavity served as the “master” mesh. Then, a registration process involving scaling was iteratively performed between each model, designated as the “fixed entity”, and the master mesh, designated as the “moving entity”. This

process aimed to scale and globally align the “master” mesh with each one of the 39 input models as closely as possible. Similarly, a Warp operation was applied between each model and the master, to create point correspondence. This operation produced, for each model, a new one that contained the same number and position of triangles in comparison to the “master”.

To validate the SSM, other SSMs were created by generating models with varying numbers of random models (30, 32, 34, 36, 38), following the same process previously described.

For the study of CFD, it has been decided to consider only a SSM of the nasal cavity to reduce computational effort and potential errors close to the sinuses’ borders. The final model, with a cylinder as an inlet and a flat trimmed surface as an outlet, is shown in *Figure 1*.

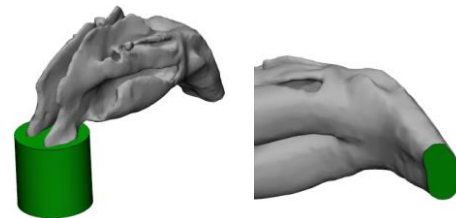


Figure 1: Boundary conditions of the cavity

3.3. CFD Simulations

For the second part of this thesis, the study of the SSM excluding the paranasal sinuses (made of 40 patients) was considered to perform CFD simulations. This choice has been made in accordance with the literature. Firstly, some refinements have been necessary, such as a stronger smoothing factor to get a better quality of the external surface. Then, since the model presented some cavities and holes, a manual repair of these imperfections was performed. The “trim” tool was used on this model to cut the end of the domain, in correspondence of the nasopharynx. At this point, a sensitivity analysis has been performed, applying meshes with edge lengths from 0.300mm to 0.175mm, as suggested by the literature. After each surface mesh, a volumetric one with tet4 elements has been introduced. These elements are 4-node tetrahedral elements that have a simple geometry with linear shape functions, making them computationally efficient.

After exporting the model as “fluent file” with surface sets, it began the set-up on Ansys (Inc., PA,

USA, 2024). The process started in Fluent, where material properties for air have been specified, and the standard $k-\epsilon$ turbulence model has been selected. Boundary conditions have been set for inlet, outlet, and walls. The SIMPLE or Coupled method has been chosen for pressure-velocity coupling, with second-order discretization. Residual monitors have been set, and the simulation was initialized using hybrid initialization before starting the calculation.

The last development of this work aimed to reproduce the introduction of an ideal sensor in one nostril, a small cylindrical component with a radius of 1.6mm and length of 10mm was subtracted from the cavity and the same process was followed. Since the sensor doesn't exist yet, geometry has been chosen as a simple geometry with realistic dimensions and three potential inclinations have been investigated: close to the upper nostril's cartilage, close to the lower one, and in a middle positioning. An example is shown in *Figure 2*.

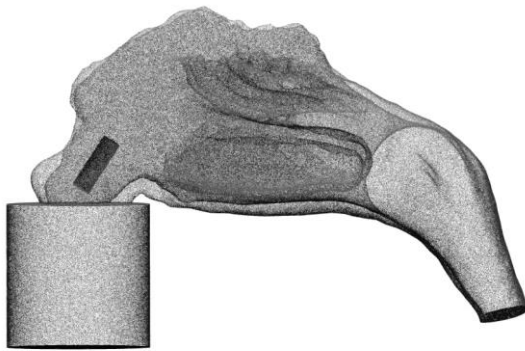


Figure 2: example of sensor positioning into the nostrils.

4. Results

4.1. Segmentation

An example of a final segmented cavity with sinuses is visible in *Figure 3*. The frontal sinus corresponds to the yellow mask, lateral to pink, ethmoidal to blue, and cavity to purple.

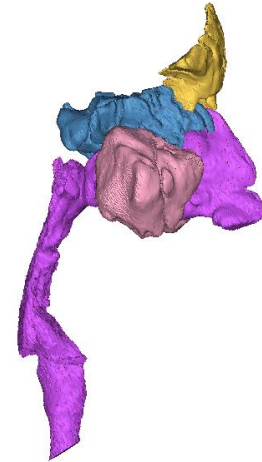


Figure 3: 3D model of a segmented cavity with paranasal sinuses

The nasopharynx is highly rough, and it can vary a lot in dimensions due to the physical characteristics of the patient and the dimensions of the CT scan. The mask that exhibits more variability is the ethmoidal sinus which is made of many small chambers of air. Moreover, their connecting walls are often difficult to capture.

4.2. Statistical Shape Modelling

The generated SSM of the complete geometry is shown in *Figure 4*.

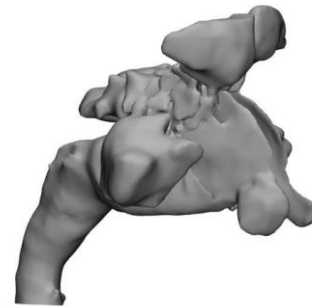


Figure 4: SSM of the nasal cavity with paranasal sinuses

The cumulative variance (CV) of each mode of the SSM made of 40 complete cavities can be seen in the properties of the model and is reported in *Figure 5* for the first 32 components, at which it reaches 95.62 %.

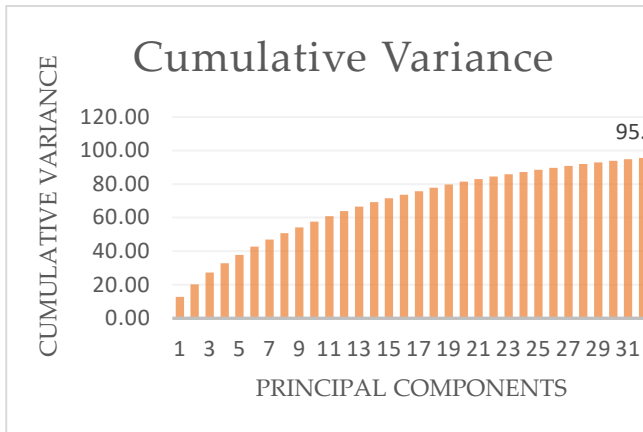


Figure 5: Cumulative Variance of SSM with paranasal sinuses

A comparison with other two studies is reported in Table 1. Despite the smaller sample size in this study, the results are consistent with comparable research, demonstrating effective model efficiency in achieving the desired CV with fewer modes.

Table 1: Comparison of CV (95%) with other studies

| Reference | Sample Size | Number of modes [95% CV] |
|------------|-------------|--------------------------|
| [4] | 46 | 46 |
| [2] | 50 | 33 |
| This study | 40 | 32 |

Moreover, an example of the Root Mean Square Error (RMS) calculated through PCA to validate the model is shown in Figure 6.

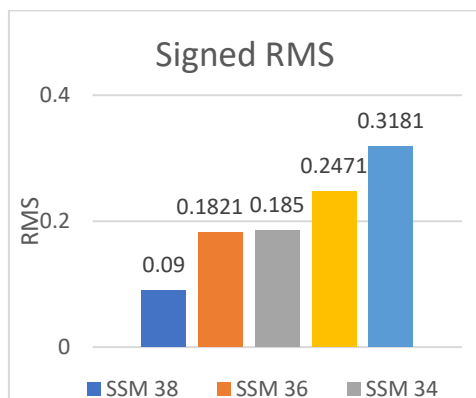


Figure 6: Signed RMS from PCA to validate SSM with paranasal sinuses

From these results, it can be stated that the SSM with paranasal sinuses is robust and consistent. As expected, its reliability increases with the number of patients considered.

4.3. CFD Simulations

From sensitivity analysis, the mesh of 0.20mm has been chosen as the optimal one. When introducing the sensor, a local refinement of 1mm has been applied.

The velocity field and the pressure distribution are reported in Figure 7 and Figure 8.

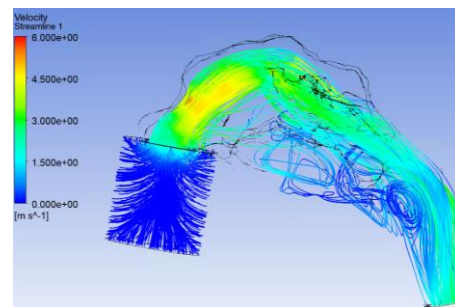


Figure 7: Velocity field of CFD simulation

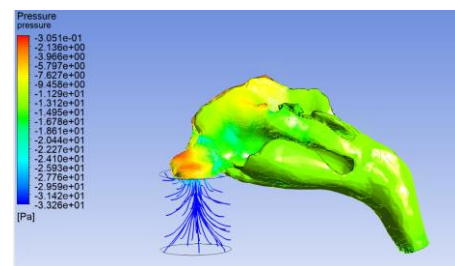


Figure 8: Pressure distribution of CFD simulation

Results from steady-state CFD simulations show that the greater values of the velocity field are reached in the upper part of the cavity, as found in the literature. The highest value is close to the superior concha. Many vortices are present through the geometry, especially in the lower concha (see Figure 9).

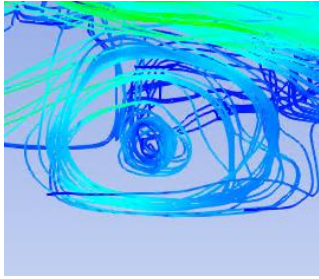


Figure 9: vortices in the lower SSM from CFD simulation

Considering that the values of pressure are measured in Pa, the drop is very small and exhibits a peak close to the nostrils.

Moreover, when introducing a sensor into the nostrils, the global velocity field changes with a maximum deviation of -4.5%. The global variation in terms of pressure remains very low (1.66%) while, along the surface of the sensor, it increases or decreases depending on its positioning. An example of a pressure distribution along the surface of the sensor is shown in the following Figure 10.

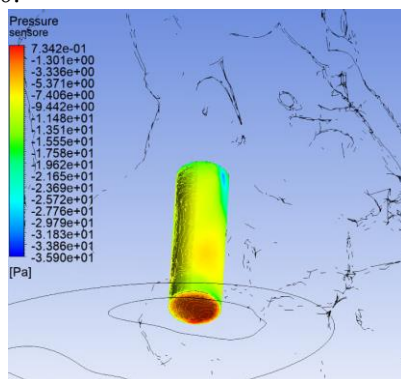


Figure 10: Example of Pressure's distribution along the sensor's surface (3rd positioning)

5. Conclusions and Future Developments

This thesis developed and validated a Statistical Shape Model of the nasal cavity with paranasal sinuses based on 40 patients. To validate the model a Part Comparison Analysis has been performed, comparing the obtained SSM with others generated from subgroups of the same dataset. The results demonstrated the model's reliability and comprehensive nature. During this process, the manual segmentation of CT scans was time-consuming and exposed to human errors, suggesting the need for automated segmentation algorithms for future research. This SSM is able to

represent a wide range of anatomical variability and has a generative power, which is crucial for medical and clinical applications.

Moreover, a second SSM was generated excluding the paranasal sinuses due to their complex geometries. According to the literature, air exchange between the nasal cavity and the surrounding chambers is negligible, making this simplification acceptable for CFD simulations. Simulations revealed that airflow velocity is greater at the superior concha and lower at the bottom of the geometry, while the peak of pressure is evident close to the nostrils and exhibits a linear trend along the cavity.

Introducing a small sensor inside one nostril, the airflow is minimally influenced, with a pressure difference of up to -1.66% and velocity variation of up to -4.5%, though local pressure around the sensor surface slightly increases or decreases depending on its positioning. Further improvements of this work could involve transient simulations, boundary layer introduction, and non-rigid walls to simulate a more realistic breathing condition. Experimental validation using 3D-printed models is the next step for future development, with potential applications not only in odour perception, but also in other fields, such as drug deposition research, surgery training, other sensors, and so on.

References

- [1] "Three dimensional modelling and automatic analysis of the human nasal cavity and paranasal sinuses using the computational fluid dynamics method," Tretiakow D, Tesch K, Meyer-Szary J, Markiet K, Skorek A..
- [2] "Characterization of the Airflow within an Average Geometry of the Healthy Human Nasal Cavity," Brüning, J., Hildebrandt, T., Heppt, W. et al..
- [3] "A new segmentation algorithm for measuring CBCT images of nasal airway: a pilot study," Zhang C, Bruggink R, Baan F, Bronkhorst E, Maal T, He H, Ongkosuwito EM..
- [4] "High quality statistical shape modelling of the human nasal cavity and applications," Keustermans W, Huysmans T, Danckaers F, Zarowski A, Schmelzer B, Sijbers J, Dirckx JJJ..

- [5] "“Statistical Shape Models - Understanding and Mastering Variation”,” Ambellan F, Lamecker H, von Tycowicz C, Zachow S..
- [6] "Computational fluid dynamics simulation of airflow in the normal nasal cavity and paranasal sinuses," Xiong GX, Zhan JM, Jiang HY, Li JF, Rong LW, Xu G..
- [7] "Numerical simulation of normal nasal cavity airflow," Tan J, Han D, Wang J, Liu T, Wang T, Zang H, Li Y, Wang X..
- [8] "Computational Fluid Dynamics Analysis of Nasal Airway Changes after Treatment with C-Expander," Xiao W, Liu S, Lu Y, Lei L, Liu N, Shen X, He Y, Liu O..